

In Situ Redispersion of Platinum Autoexhaust Catalysts: An On-Line Approach to Increasing Catalyst Lifetimes?*

Yasutaka Nagai,* Kazuhiko Dohmae, Yasuo Ikeda, Nobuyuki Takagi, Toshitaka Tanabe, Naoyuki Hara, Gemma Guilera, Sakura Pascarelli, Mark A. Newton, Oji Kuno, Hongying Jiang, Hirofumi Shinjoh, and Shin'ichi Matsumoto

Dedicated to the Catalysis Society of Japan on the occasion of its 50th Anniversary

Supported precious metals, such as platinum (Pt), rhodium (Rh), and palladium (Pd), are used to facilitate many industrial catalytic processes. Pt in particular is found at the core of catalysts used throughout the petrochemical industry: from bifunctional catalysts (isomerization/dehydrogenation) used for refining of hydrocarbon fuel stocks, to three-way (CO and hydrocarbon oxidation/ NO_x reduction) conversions within car exhausts. In this latter, ubiquitous application—commercialized in the USA and Japan in 1977^[1]—Pt has always been a pivotal component in the abatement of harmful gas emissions from gasoline- or diesel-driven engines. The ever-increasing appreciation of the damage that noxious gas emissions are doing to our environment and the finite availability of noble metals provide strong drivers for the continued study and optimization of the behavior of Pt-based three-way catalysts (TWCs). Central to technological progress in this area is a fundamental understanding of how these materials behave, which may allow us to stop them degrading or deactivating during operation.

A longstanding problem, affecting many applications that use highly dispersed metal nanoparticles, is loss of active surface area in the metal components as a result of “sintering”. This is a particularly pernicious problem in applications in which catalysts have to experience high temperatures—in excess of 800 °C in the case of modern car catalysts. This deleterious process causes the particle size of the metal to increase massively—through either particle diffusion or agglomeration or through “ripening” processes. The result is that a large fraction of the active metal is effectively “hidden away” within the bulk of these larger particles where it cannot be used to affect the desired chemical conversions that occur on the particle surface.

This central issue of exhaust catalyst deactivation has long been recognized in the hydrocarbon reforming^[2] and emission abatement industries.^[3] In the former industry, “oxidative redispersion” has been utilized to reverse the effects of sintering and regenerate spent Pt-based reforming catalysts. However, whereas other noble metal particles such as Pd or Rh can be effectively redispersed by gaseous oxygen at certain temperatures,^[4] this method is efficient for Pt catalysts only when Cl is present either in the catalyst formulation or as an adjunct added during the redispersion process: in the absence of Cl, redispersion in Pt/ Al_2O_3 by oxygen is limited both to a narrow temperature window (of around 500 °C) and a low level of redispersion.^[5,6] Further, a continuous oxidative treatment over time is required for this redispersion process. Exhaust gases exiting from gasoline engines change quickly and dramatically during operation. Temperatures can rise transiently to around 1000 °C, and the exhaust gas composition itself fluctuates quickly between oxidative and reductive compositions. Clearly, the conventional approach to redispersion and reactivation is highly unsuitable on many counts for “on-board” redispersion and regeneration of TWCs.

Other regeneration phenomena have recently been shown in some related cases. The “intelligent” catalyst system of Daihatsu shows in-built structural reversibility of the noble metal component.^[7] In this case, it is the structure of the perovskite support that provides the foundation for this extremely elegant piece of applied catalyst design. The possibility of forming very large particles is intrinsically reduced and, under some circumstances, this technology has been successfully commercialized. However, this approach is very much dependent upon the structure of a particular and low surface area support material and is limited in this sense.

[*] Dr. Y. Nagai, K. Dohmae, T. Tanabe, Dr. H. Shinjoh

TOYOTA Central R&D Labs., Inc.

Nagakute, Aichi 480-1192 (Japan)

Fax: (+81) 561-63-6150

E-mail: e1062@mosk.tytlabs.co.jp

Y. Ikeda, N. Hara

TOYOTA Motor Europe Technical Centre, Zaventem (Belgium)

N. Takagi

Higashi-Fuji Technical Center, TOYOTA Motor Corporation

Shizuoka (Japan)

Dr. G. Guilera, Dr. S. Pascarelli, Dr. M. A. Newton

European Synchrotron Radiation Facility, Grenoble (France)

O. Kuno, Dr. H. Jiang

TOYOTA Motor Engineering & Manufacturing North America, Inc.,

Michigan (USA)

Dr. S. Matsumoto

TOYOTA Motor Corporation, Toyota, Aichi (Japan)

[**] We are grateful to Bernard Gorges, Olivier Mathon, Sebastien Pasternak, Florian Perrin, Steven Fiddy (ESRF), Muriel Lepage, Takashi Kuzuya (TOYOTA Motor Europe), Takamasa Nonaka, Satoshi Yamaguchi, Naoki Takahashi, Yoshiki Seno (TOYOTA Central R&D), Paul Fanson (TOYOTA Motor NA), Takeshi Hirabayashi, Masahide Miura, and Keisuke Kishita (TOYOTA Motor corporation) for their excellent work.



Supporting information for this article is available on the WWW under <http://dx.doi.org/10.1002/anie.200803126>.

A rapid, reversible, but non-oxidative sintering/redispersion cycle in supported Pd nanoparticle catalysts has also recently been shown.^[8] However, although this approach appears to be support-independent^[9] and intrinsic to small (< 3 nm) Pd nanoparticles, it is unknown whether such chemistry is possible when starting with much larger metallic entities or with other noble metals such as Pt or Rh.

Herein, we show, through the application of in situ and time-resolved X-ray absorption spectroscopy (XAS) and in situ transmission electron microscopy (TEM), the rapid and effective redispersion of Pt particles up to around 10 nm in diameter on ceria-based oxide supports during redox cycling. The foundation for this behavior lies in the nature of the Pt–ceria interaction, and it is shown to proceed through atomic migration rather than particle coalescence/splitting. Most importantly, the thermo-kinetic character of this process, as revealed by time-resolved spectroscopy and microscopy, does have tangible potential for incorporation into an “on-board” methodology for extending car catalyst lifetime through curtailing or reversing the effects of metal sintering during operation.

In the current case, real-time observation of changes in noble-metal structure were made at the Pt L_{III} edge by using the fluorescence yield variant (Turbo-XAS) of energy-dispersive XAS developed by Pascarelli et al. at ID24 of the European Synchrotron Radiation Facility (ESRF).^[10] The combination of low levels of Pt in the catalysts and high levels of heavy, absorbing, elements such as Ce and Zr severely compromises conventional, transmission-based, dispersive XAS experiments. Therefore, to obtain a window into the structure–reactivity behavior of the Pt in these systems with a suitable time resolution, the fluorescence variant needs to be adopted as it permits the measurement of Pt L_{III} edge X-ray absorption near-edge structure (XANES) on the timescale required for these taxing samples.^[11]

In this work, 2 wt % Pt/Al₂O₃ and 2 wt % Pt/CeZrY mixed oxide (referred to as CZY) catalysts were prepared. Figure 1 shows the variation of the white-line peak height of the normalized Pt L_{III} edge XANES for the fresh Pt/Al₂O₃ and Pt/CZY catalysts under cyclic oxidizing/reducing conditions at 400–800 °C. Gas mixtures of 4 or 20 % O₂/He and 3 % H₂/He gas were introduced alternately into the cell every 60 s. The gas flowing over the sample was quickly between an oxidative and reductive atmosphere by using a gas-actuated switching valve (Figure S1 in the Supporting Information). Pt L_{III} edge XANES spectra were collected approximately every 6 s. Reasonable quality data for both catalysts could be collected by using Turbo-XAS in fluorescence mode (Figure S2 in the Supporting Information). Under a reductive atmosphere, the supported Pt catalyst is in a metallic state and the white-line peak is small; in contrast, under oxidative atmosphere, the surface of Pt particles can be oxidized, and the white-line peak is high (inset in Figure 1a). ΔI in Figure 1 denotes the difference between the white-line peak heights of the oxidized and reduced samples. Since the white-line peak height of the reduced sample is constant, the height of the oxidized catalyst is proportional to ΔI . In a previous experiment, we found that the value of ΔI increased with the decreasing particle size of Pt.^[11] This result was confirmed by

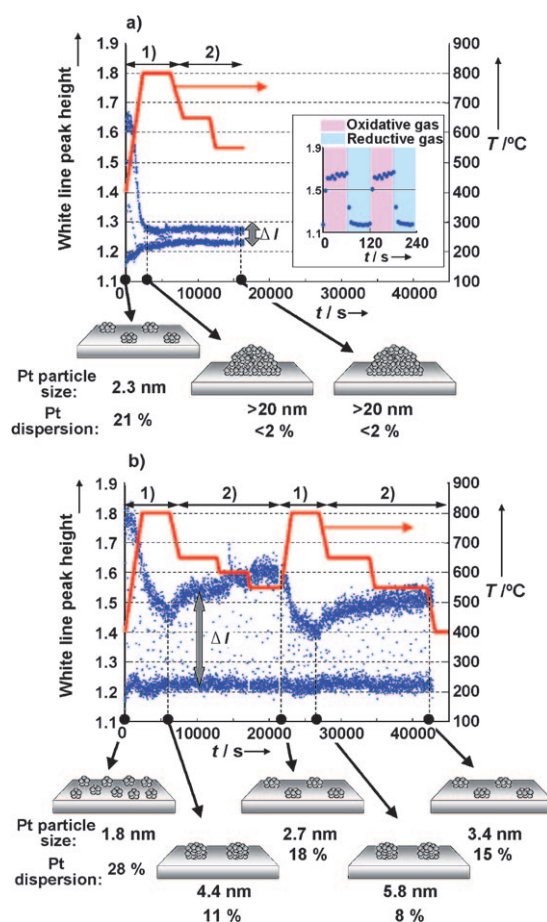


Figure 1. Temporal dependence of the white-line peak height of the Pt L_{III} edge in XANES for fresh a) Pt/Al₂O₃ and b) Pt/CZY catalysts under oxidizing/reducing atmospheres at 400–800 °C and a schematic representation of the sintering/redispersion behavior. 1) 4 % O₂/He and 3 % H₂/He gases, 2) 20 % O₂/He and 3 % H₂/He gases were alternately introduced into the cell every 60 s throughout the measurement. Inset: Magnified view of initial stage of the experiment.

the good relationship between the Pt particle size measured by CO pulse adsorption method and ΔI (Figure S3 in the Supporting Information). Therefore, it is possible to track the change in Pt particle size during in situ redox cycling. In Figure 1a, for Pt/Al₂O₃, ΔI is seen to decrease as the temperature is increased, and then ΔI is constant as the temperature is decreased. Using the correlation between the Pt particle size and ΔI , we observed that only facile sintering of Pt particles (> 20 nm) occurred in the Pt/Al₂O₃ sample, and Pt redispersion was not seen at any temperature. This situation is dramatically different for Pt/CZY. In Figure 1b, ΔI decreases as the temperature is increased. Upon lowering the temperature ΔI gradually increases. This result indicates that the average Pt particle size becomes correspondingly larger or smaller as a function of the temperature. The Pt particle size of the fresh catalyst increases from 1.8 to 4.4 nm during the temperature ramp from 400 to 800 °C, but then decreases to 2.7 nm as the temperature is lowered to 550 °C. It is interesting to note that the sintering/redispersion phenomena can be reversibly controlled by the sample temperature. During redispersion, the Pt particle size recovers from 4.4 to

2.7 nm at first, and then from 5.8 to 3.4 nm. The driving force behind this Pt redispersion on CZY is attributed to the strong interaction between the Pt oxide and the ceria support under an oxidative atmosphere.^[12]

The effect of initial Pt particle size on the speed of Pt redispersion was investigated. Pre-aged, and therefore sintered, Pt/CZY catalysts were used for this redispersion experiment. Figure 2a–e shows the variation of the white-line peak height for the preliminary sintered Pt/CZY samples.

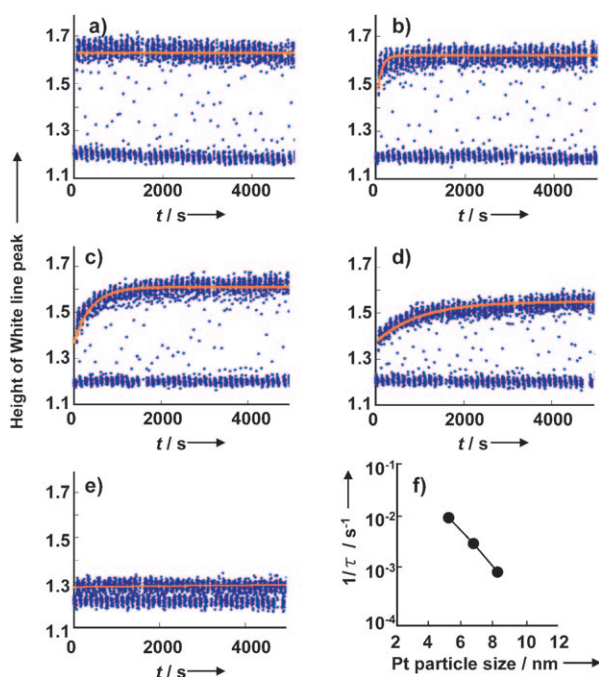


Figure 2. Temporal dependence of the white-line peak height of Pt L_{III} edge in XANES for pre-aged Pt/CZY with Pt particle sizes (by CO pulse method) of a) 3.1 nm, b) 5.2 nm, c) 6.7 nm, d) 8.2 nm, and e) 12.2 nm. f) Correlation between the Pt redispersion speed ($1/\tau$) and the initial Pt particle size. Gas mixtures of 20% O_2/He and 3% H_2/He were introduced alternately into the cell every 60 s at 600°C.

20% O_2/He and 3% H_2/He gases were alternately introduced every 60 s at 600°C. The ΔI curve was simulated by an exponential function [Eq. (1)], in which ΔI_i and ΔI_f are the initial and final values of ΔI , respectively, t is time (in seconds), and τ is the time constant.

$$\Delta I = \Delta I_f - (\Delta I_f - \Delta I_i) \exp(-t/\tau) \quad (1)$$

The results of the simulations are also shown (orange lines in Figure 2). In this case, $1/\tau$ defines the speed of Pt redispersion; the correlation between $1/\tau$ and the initial Pt particle size (for particle sizes in the range 5.2–8.2 nm) is plotted in Figure 2 f. This result indicates that increasing the Pt particle size decreases the speed of Pt redispersion.

Additionally, the effect of temperature on the speed of Pt redispersion was investigated in the same way as the study of Pt particle size (Figure S4 in the Supporting Information). A pre-aged Pt/CZY catalyst (Pt particle size of 6.7 nm from CO pulse method) was used for this experiment. 20% O_2 and 3%

H_2 gases were alternately introduced every 60 s at 500, 600, and 700°C. An increased temperature yields an increased speed of redispersion, showing that Pt redispersion is an activated process. Additionally, ΔI does not change under repeated redox cycling at 400°C, which indicates that high temperatures of 500°C and above are required for the Pt redispersion. The effect of O_2 concentration on Pt redispersion was also investigated (Figure S5 in the Supporting Information), and the results show that an increased rate of redispersion is also achieved with increasing O_2 concentration up to 20%.

To verify the veracity of the XAS-based measurements, and to establish the mechanism of these events, in situ TEM observations were performed on the Pt/CZY sample. Figure 3 shows snapshots of the progression of structural changes as

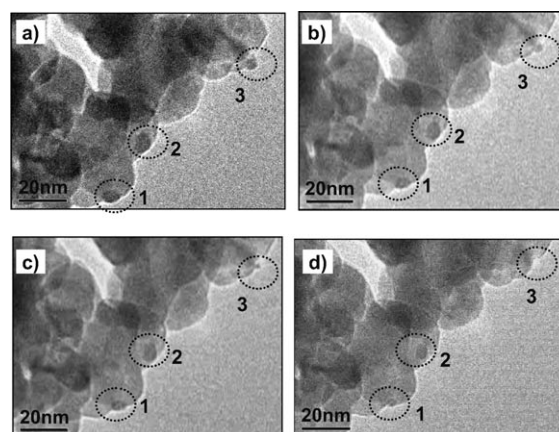


Figure 3. In situ TEM images of the Pt redispersion process for a pre-aged Pt/CZY sample (Pt particle size 6.7 nm by CO pulse method). Images were recorded at a pressure of 1.3 kPa O_2 at 820°C a) at the start of the experiment, and after b) 1.5 min, c) 3 min, and d) 6 min. Circles 1–3 indicate Pt metal particles.

viewed by TEM during the redispersion of Pt particles (of average starting size 6.7 nm) under 1.3 kPa O_2 at 820°C. A complete in situ TEM movie can be found as Movie S1 in the Supporting Information. The Pt particles (1 and 2) decreased in size greatly, and Pt particle in the circle 3 disappeared completely. The temporal dependences of the Pt particle size are shown in Figure S6 of the Supporting Information. In the TEM movie, the Pt sintering could not be observed in this field of view. Therefore, this movie captured the Pt redispersion process. It should be noted that no crystallite migration and splitting were observed under these conditions.

Two mechanistic models have been proposed for the Pt sintering/redispersion processes.^[6] The first envisages the sintering/redispersion to occur by migration or splitting of the crystallites. In this mechanism, the sintering occurs by migration, collision, and coalescences of metal crystallites on the support surface,^[14] and redispersion takes place by splitting of the crystallites into smaller particles.^[15] The second model envisages the sintering/redispersion to occur by dissociation of molecular or atomic species from the metal crystallites and subsequent migration and capture of these species on the support surface (redispersion) or other metal

crystallites (sintering).^[16,17] Whereas the XAS measurements do not, a priori, distinguish between these two mechanistic possibilities, the in situ TEM results appear quite definitive in favoring the atomic migration model. Moreover, the atomic migration model can predict decreases and increases in dispersion depending on the treatment and the PtO–support interaction through consideration of the following aspects of the thermodynamic equilibrium.

In Equation (2), the (s) indicates Pt species trapped on the



support surface. The stability of $\text{PtO}_x(\text{s})$ will depend on the PtO–support interaction. The $\text{Pt}(\text{s})$ species easily move on the support surface and will be captured by other Pt metal particles. In the case of $\text{Pt}/\text{Al}_2\text{O}_3$, because the interaction between Pt and Al_2O_3 is weak, $\text{PtO}_x(\text{s})$ readily decomposes to form $\text{Pt}(\text{s})$ species, and then Pt sintering occurs dominantly. Pt redispersion for the sintered Pt particles (> 20 nm) on Al_2O_3 support never occurs under the conditions employed in this study. For the Pt/CZY catalyst, oxygen is adsorbed on the surface of sintered Pt particles to form mobile Pt oxide species. As Pt oxide species trapped on the ceria surface are stable enough, redispersion and sintering may occur reversibly. The $\text{PtO}_x(\text{s})$ species can be stabilized at lower temperature and a high concentration of O_2 , and effective redispersion proceeds. By contrast, sintering prefers low O_2 concentration and high temperature. Of course, high temperature accelerates the Pt redispersion speed at temperatures where the $\text{PtO}_x(\text{s})$ species are stable. In addition, large Pt particles decrease the Pt redispersion speed even if temperature and O_2 concentration were in a favorable range for redispersion, because the decreased surface area of large Pt particles significantly decreases the generation speed of $\text{PtO}_x(\text{s})$. On the basis of this notion, the sintering and redispersion in Pt/CZY could be observed reversibly with the change of temperature, O_2 concentration, and Pt particle size. With this paradigm, we might suggest that a component of the “real-world” deterioration of such catalysts may result from repeated sintering and redispersion cycles alongside more well known temperature “ripening” processes.

Finally, an overall scheme of Pt/CZY redispersion within a cyclical redox situation, and based on in situ TEM observations and kinetic results by XAS, is suggested (Figure S7 in the Supporting Information): Oxygen is adsorbed on the surface of large Pt particles and some mobile Pt oxide species form, migrate, and are trapped on the support surface through a relatively strong the PtO–support interaction. Under reducing conditions, the PtO–Ce bond in the CZY support breaks and Pt oxides are reduced to Pt metal, and thus new small particles of Pt metal are formed. In our previous study, we confirmed the formation and cleavage of the PtO–Ce bond in CZY by EXAFS analysis.^[12] The Pt redispersion process proceeds by the repetition of the atomic migration of Pt oxide from the surface of large metal particles and the reduction of PtO–support species.

Experimental Section

Al_2O_3 as a support oxide was supplied by Nikki Universal Co., Ltd.; its crystal structure is gamma-type. The CeZrY mixed oxide (referred to as CZY) support was prepared by a coprecipitation process with aqueous NH_3 using $\text{Ce}(\text{NO}_3)_3$, $\text{ZrO}(\text{NO}_3)_2$, and $\text{Y}(\text{NO}_3)_3$ in aqueous solutions. The precipitate was dried and calcined in air at 700°C for 3 h. CZY oxide contains 50 wt % CeO_2 , 46 wt % ZrO_2 , and 4 wt % Y_2O_3 ; its crystal structure is cubic. Catalysts with 2 wt % Pt on Al_2O_3 and 2 wt % Pt on CZY were prepared by the conventional wet impregnation of support powders with an aqueous solution of $[\text{Pt}(\text{NH}_3)_2(\text{NO}_2)_2]$. Portions of the fresh Pt/CZY powders were aged in 3 % H_2/He or N_2 at various temperatures to obtain specifically sized particles of sintered Pt. The average particle size of Pt metal was measured by the CO pulse adsorption method. CO pulse adsorption was carried out in flowing He at -78°C . At this temperature, the CO uptake on the ceria support was almost entirely suppressed, and CO was adsorbed only to the surface of Pt.^[13] Real-time observation of the sintering/redispersion behavior of Pt was made possible by in situ time-resolved Turbo-XAS (T-XAS) in fluorescence mode at ID24 (ESRF).^[10] Pt L_{III} edge XAS spectra were collected every 1.1–6.0 s. In situ TEM measurements were carried out at around 820°C in 1.3 kPa O_2 .

Received: June 30, 2008

Published online: October 10, 2008

Keywords: electron microscopy · heterogeneous catalysis · platinum · time-resolved spectroscopy · X-ray absorption spectroscopy

- [1] S. Matsumoto, *Catal. Today* **2004**, 90, 183–190.
- [2] J. A. Anderson, M. G. V. Mordente, C. H. Rochester, *J. Chem. Soc. Faraday Trans. 1* **1989**, 85, 2983–2990.
- [3] R. A. Dalla Betta, T. Rostrup-Nielsen, *Catal. Today* **1999**, 47, 369–375.
- [4] H. Lieske, J. Völter, *J. Phys. Chem.* **1985**, 89, 1841–1842.
- [5] R. M. J. Fiedorow, B. S. Chahar, S. E. Wanke, *J. Catal.* **1978**, 51, 193–202.
- [6] R. M. J. Fiedorow, S. E. Wanke, *J. Catal.* **1976**, 43, 34–42.
- [7] a) Y. Nishihata, J. Mizuki, T. Akao, H. Tanaka, M. Uenishi, M. Kimura, T. Okamoto, N. Hamada, *Nature* **2002**, 418, 164–167; b) H. Tanaka, M. Taniguchi, M. Uenishi, N. Kajita, I. Tan, Y. Nishihata, J. Mizuki, K. Narita, M. Kimura, K. Kaneko, *Angew. Chem.* **2006**, 118, 6144–6148; *Angew. Chem. Int. Ed.* **2006**, 45, 5998–6002.
- [8] M. A. Newton, C. Belver-Coldeira, A. Martínez-Arias, M. Fernández-García, *Nat. Mater.* **2007**, 6, 528–532.
- [9] M. A. Newton, C. Belver-Coldeira, A. Martínez-Arias, M. Fernández-García, *Angew. Chem.* **2007**, 119, 8783–8785; *Angew. Chem. Int. Ed.* **2007**, 46, 8629–8631.
- [10] S. Pascarelli, T. Neisius, S. De Panfilis, *J. Synchrotron Radiat.* **1999**, 6, 1044–1050.
- [11] Y. Nagai, N. Takagi, Y. Ikeda, K. Dohmae, T. Tanabe, G. Guileria, S. Pascarelli, M. A. Newton, H. Shinjoh, S. Matsumoto, *AIP Conf. Proc.* **2007**, 882, 594–596.
- [12] Y. Nagai, T. Hirabayashi, K. Dohmae, N. Takagi, T. Minami, H. Shinjoh, S. Matsumoto, *J. Catal.* **2006**, 242, 103–109.
- [13] A. Holmgren, B. Andersson, D. Duprez, *Appl. Catal. B* **1999**, 22, 215–230.
- [14] E. Ruckenstein, B. Pulvermacher, *J. Catal.* **1973**, 29, 224–245.
- [15] P. Wynblatt, N. A. Gjostein, *Scr. Metall.* **1973**, 7, 969–975.
- [16] P. C. Flynn, S. E. Wanke, *J. Catal.* **1974**, 34, 390–399.
- [17] P. C. Flynn, S. E. Wanke, *J. Catal.* **1974**, 34, 400–410.